Characteristics of Atmospheric Microplasma in Small Discharge Gaps

Marius Blajan and Kazuo Shimizu

Organization for Innovation and Social Collaboration, Shizuoka University,

3-5-1 Jyouhoku, Hamamatsu, 432-8561, JAPAN. E-mail : blajanmarius@yahoo.com

Introduction

Microplasma can be found in many applications. In the last years, the technology was used in applications such as NOx removal, surface treatment and sterilization or inactivation of bacteria. The fundamental phenomena of microplasma are not fully understood. Emission spectroscopy, imaging and Stark broadening techniques were used to clarify the characteristics of microplasma. Due to the small discharge gaps our microplasma could be analyzed only using these non invasive methods.

Experimental Setup

(1)Microplasma Electrodes

The electrodes consist in perforated metallic plates covered with a dielectric layer.

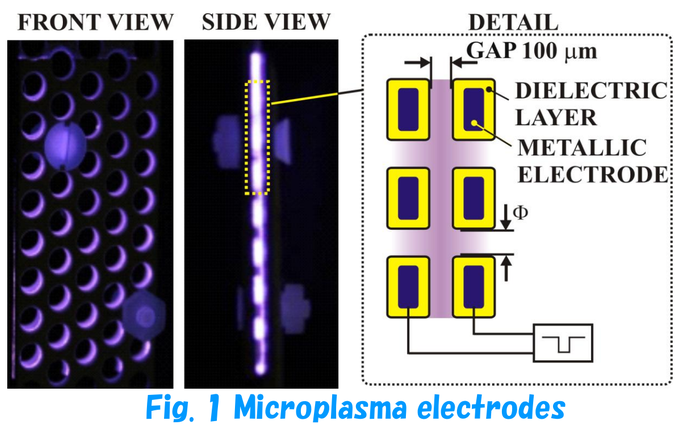

Fig. 1 Microplasma electrodes

Electrode size was 20 mm versus 40 mm for emission spectroscopy analysis. Discharge gap was set at 100 μm in this study.
A *Marx Generator* with MOSFET switches as pulse power supply:
- Output Voltage: -2 kV negative
- Rise time: 40 ns
- Pulse width: 1 μs

(2) Experimental setup

Emission spectrum was measured by a spectrometer, and an ICCD camera. Photos of microdischarges were taken using a microscope and a digital camera.
Gas flow rate: Ar and N_2/Ar at 10 L/min.

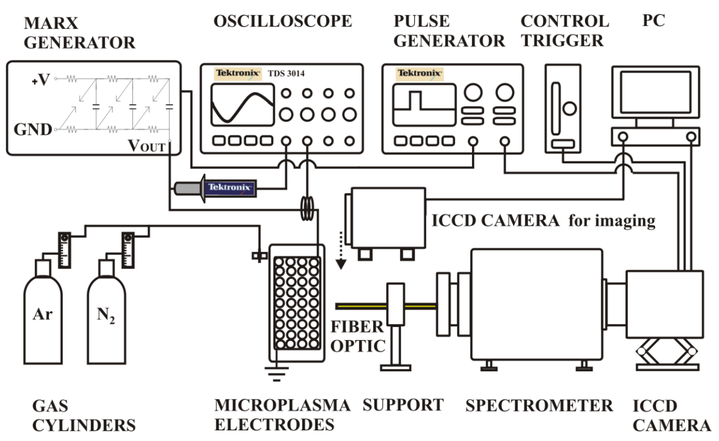

Fig. 2 An experimental setup.

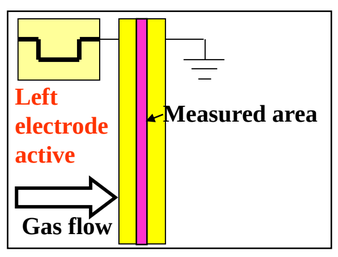

Fig. 3 Measured area of emission spectra.

(3) Microdischarges

Very small discharge gaps and relatively *low discharge voltages* (about 1 kV). A *high intensity electric field* (10^7-10^8 V/m) assures the formation of microplasma.

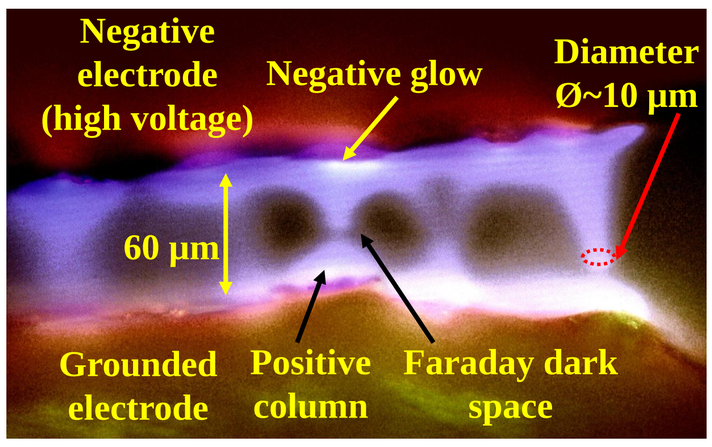

Fig. 4 Images of microdischarges phenomena.

Stark Broadening

A pseudo Voigt function was used to determine Lorentzian FWHM of the Ar I peak at 696.5 nm.

$$V(\lambda) = V_0 + S(m_u \frac{2}{\pi} \frac{L_W}{4(\lambda-\lambda_0)^2 + L_W^2} +$$

$$(1-m_u)\frac{\sqrt{4\ln 2}}{\sqrt{\pi}G_W}\exp(-\frac{4\ln 2}{G_W^2}(\lambda-\lambda_0)^2)$$

Gw is Gaussian FWHM, Lw is Lorentzian FWHM, λ is the wavelength, λ_0 is the centroid wavelength. Calculated Lw=0.0042564 nm and considering van der Waals broadening Ww= 0.003 nm → Stark width Sw=0.0012564 nm.

$$S_W = 2(1+1.75*10^{-4}*\sqrt[4]{Ne}*\alpha*$$

$$(1-0.0068*\sqrt[6]{Ne}\frac{1}{\sqrt{Te}}))*10^{-16}*w*Ne$$

For electron temperature Te=10000 → electron density Ne=1.338*10^{15} /cm^3.

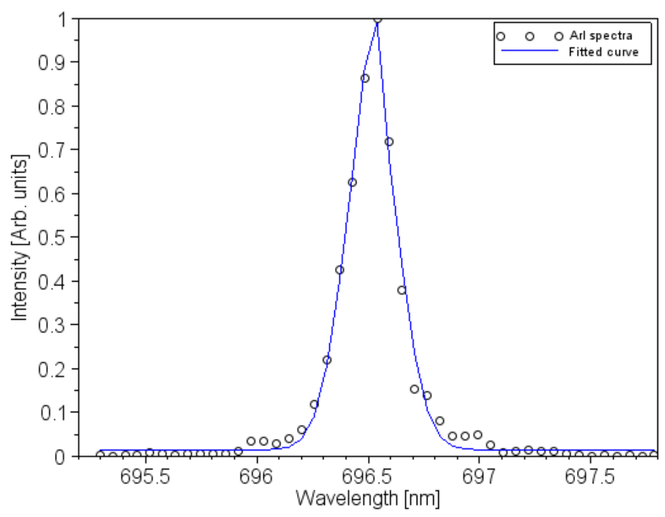

Fig. 5 Measured and fitted spectra of Ar I peak at 696.5 nm .

Spatial and temporal distribution of Ar I peak at 696.5 nm and N_2 SPS peak at 337.1 nm shows higher intensity towards anode up to 20 ns and after that shifted to cathode.

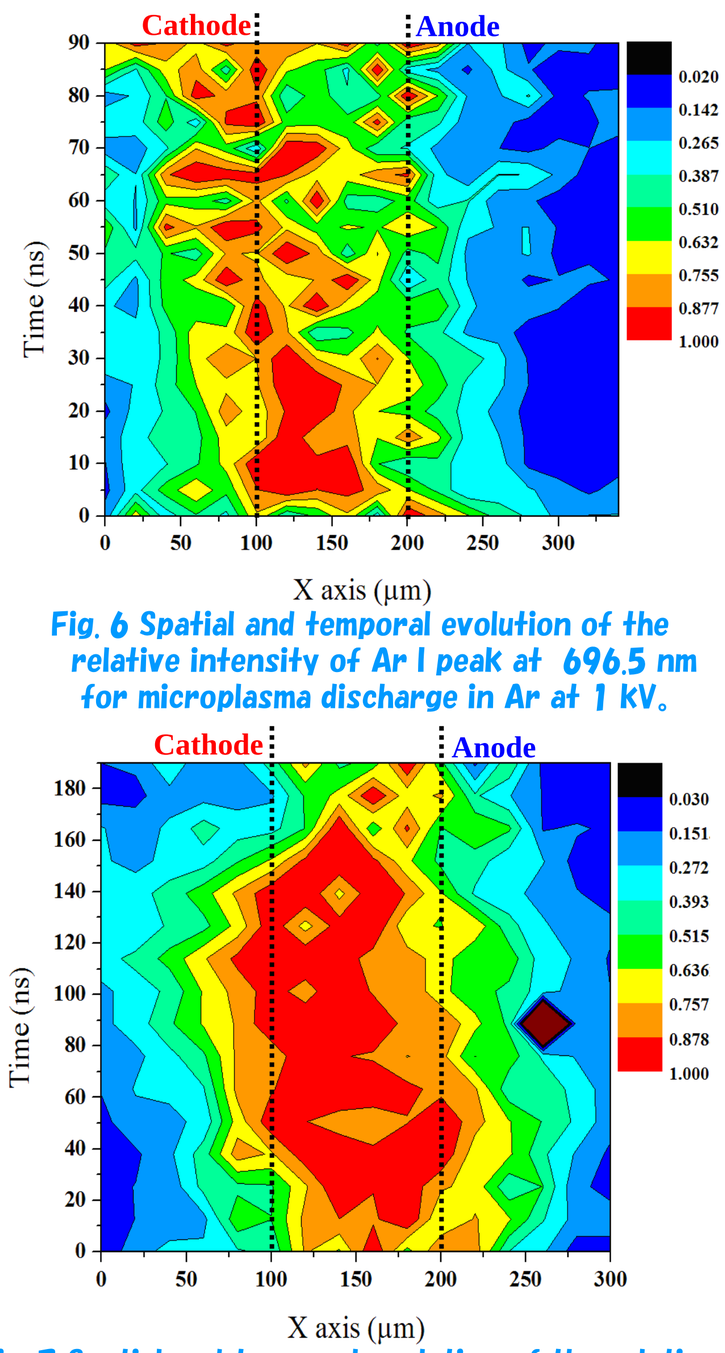

Fig. 6 Spatial and temporal evolution of the relative intensity of Ar I peak at 696.5 nm for microplasma discharge in Ar at 1 kV.

Fig. 7 Spatial and temporal evolution of the relative intensity of N_2 SPS peak at 337.1 nm for microplasma discharge in 1% N_2 in Ar at 1 kV.

Spatial and Temporal Evolution of Microplasma

The observation of microdischarge by ICCD camera shows the streamer formation and the correlation of the microdischarge evolution with the discharge current.

Discharge voltage and corresponding discharge current

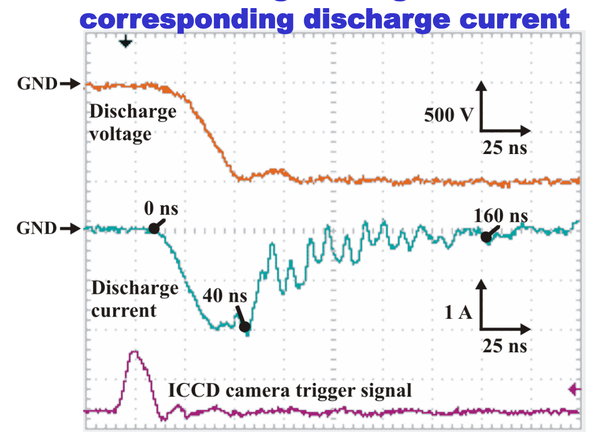

1) Streamer reaches cathode up to 1 ns

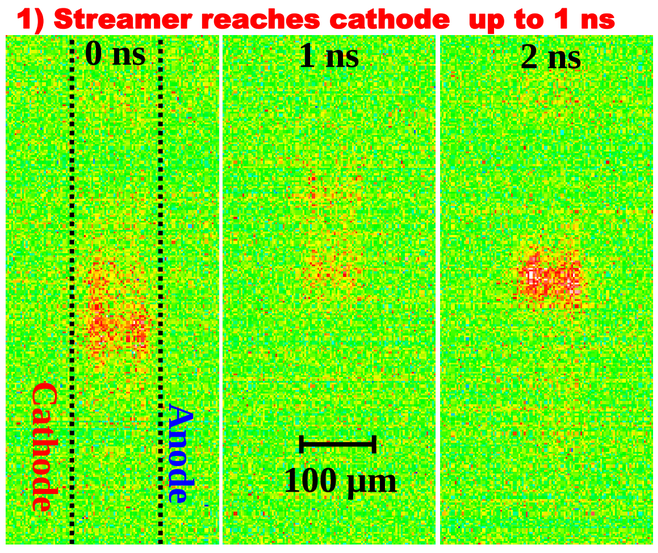

2) Cathode layer formation up to 30 ns

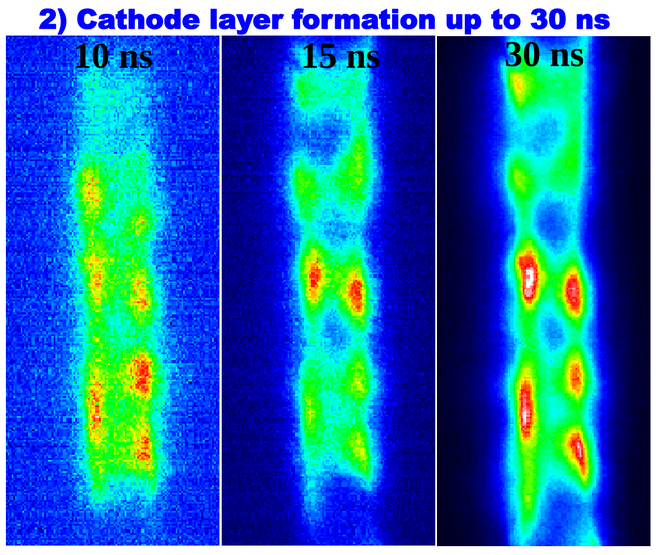

3) Cathode layer enhancement up to 70 ns

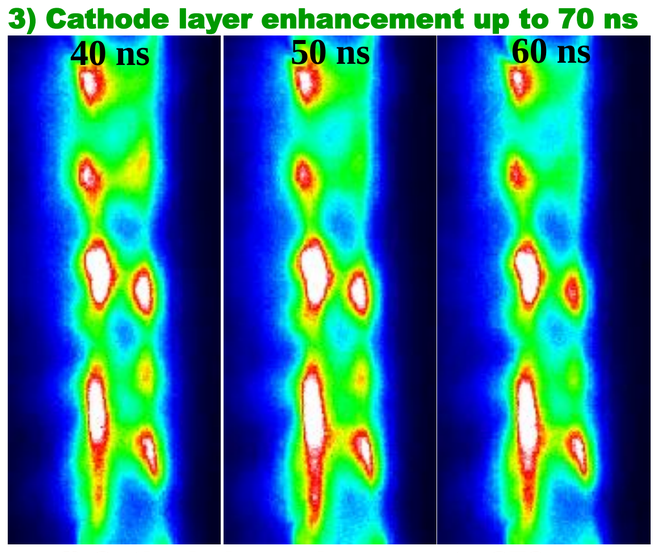

4) Cathode layer decay up to 270 ns

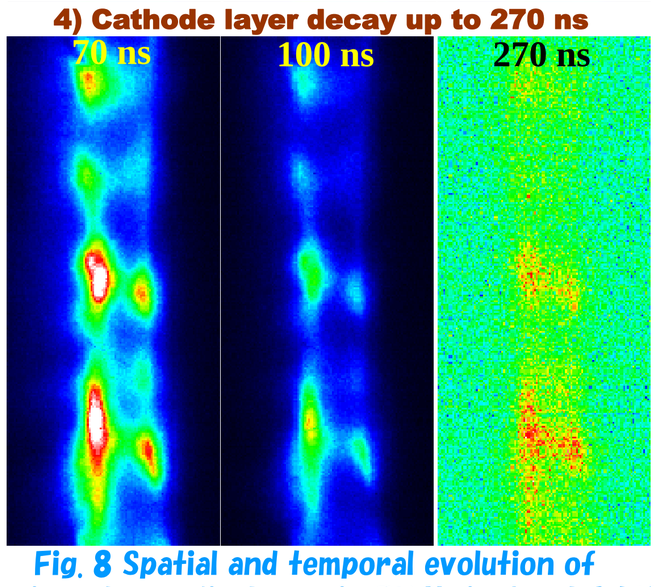

Fig. 8 Spatial and temporal evolution of microplasma discharge in 3% N_2 in Ar at 1 kV . ICCD camera shutter was opened for 2 ns.

Conclusions

- Stark broadening was used for calculating electron density and estimated to be Ne=1.338*10^{15} /cm^3.
- Spatial and temporal evolution of the relative intensities of *ArI* peak at *696.5 nm* and *N_2 SPS* peak at *337.1 nm* showed higher intensity towards anode up to 20 ns and after it shifted towards cathode.
- ICCD camera images showed the evolution of microdischarges from the phase when streamer reaches anode to cathode layer formation, cathode layer enhancement and finally cathode layer decay.